

# Dynamic Divide-and-Conquer Adversarial Training for Robust Semantic Segmentation

Xiaogang Xu<sup>1</sup>, Hengshuang Zhao<sup>1</sup>, and Jiaya Jia<sup>1,2</sup>

<sup>1</sup> The Chinese University of Hong Kong   <sup>2</sup> SmartMore  
{xgxu, hszhao, leojia}@cse.cuhk.edu.hk

**Abstract.** Adversarial training is promising for improving robustness of deep neural networks towards adversarial perturbation, especially on classification tasks. Effect of this type of training on semantic segmentation, contrarily, just commences. We make the initial attempt to explore the defense strategy on semantic segmentation by formulating a general adversarial training procedure that can perform decently on both adversarial and clean samples. We propose a dynamic divide-and-conquer adversarial training (DDC-AT) strategy to enhance the defense effect, by setting additional branches in the target model during training, and dealing with pixels with diverse properties towards adversarial perturbation. Our dynamical division mechanism divides pixels into multiple branches automatically, achieved by unsupervised learning. Note all these additional branches can be abandoned during inference and thus leave no extra parameter and computation cost. Extensive experiments with various segmentation models are conducted on PASCAL VOC 2012 and Cityscapes datasets, in which DDC-AT yields satisfying performance under both white- and black-box attack.

**Keywords:** Adversarial Training · Semantic Segmentation · Robust CNNs

## 1 Introduction

Recent work has revealed that deep learning models, especially in classification tasks, are often vulnerable to adversarial samples [21,8,19]. Adversarial attack can deceive the target model by generating crafted adversarial perturbations on original clean samples. Such perturbations are often imperceptible. Such threat also exists in semantic segmentation [26,16,1]. As shown in Fig. 1, on various datasets, state-of-the-art segmentation models [30,4] can be easily fooled by adversarial perturbation, causing poor performance on these adversarial regions.

There is seldom work to improve the robustness of semantic segmentation networks. As a universal approach, *adversarial training* [8,13,15] is effective to enhance the target model in classification by training models with adversarial samples. In this paper, we study the effect of adversarial training on the semantic segmentation task. We find that adversarial training impedes convergence on clean samples, which also happens in classification. Thus we set our goal as making networks perform well on adversarial examples and meanwhile maintaining good performance on clean samples.

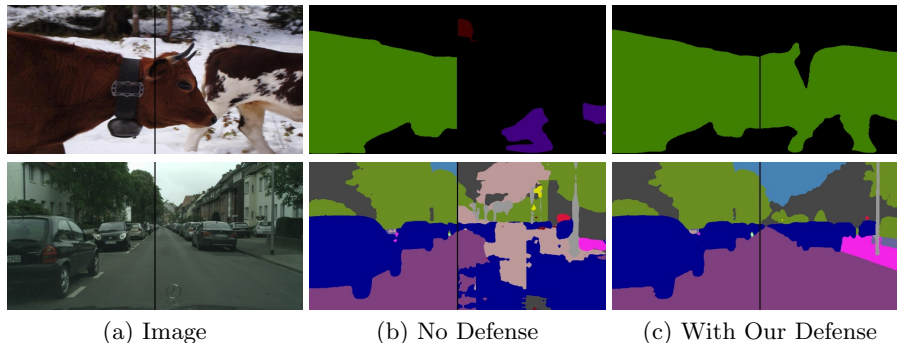


**Fig. 1.** For each image in (a), the left side is the normal data while the right side is perturbed by adversarial noise. (b) shows that adversarial attack could fail existing segmentation models. We provide an effective defense strategy shown in (c). The top and bottom rows are results with structure of PSPNet and DeepLabv3 respectively.

For semantic segmentation task, each pixel has one classification output. Thus the property of every pixel in one image toward adversarial perturbation might be different. Based on this motivation, we design a dynamic divide-and-conquer adversarial training (DDC-AT) strategy. We propose to use multiple branches in the target model during training, each handling pixels with a set of properties. During training, a “main branch” is adopted to deal with pixels from adversarial samples and pixels from clean samples that are not likely to be perturbed; an “auxiliary branch” is utilized to deal with pixels from clean samples that are sensitive to perturbations.

Moreover, such divide-and-conquer setting is dynamical. During training, pixels stay near the decision boundary from clean samples are initially set to the “auxiliary branch”. They become more insensitive to perturbation in the network, and finally move back to the “main branch” for processing. Such dynamical procedure is implemented by training a “mask branch” via unsupervised learning. With this mechanism, our method reduces performance deterioration over clean samples. Experiments manifest that such mechanism also improves robustness towards adversarial samples. Another notable advantage of our proposed DDC-AT is that branches apart from the main one can be abandoned during inference. Thus parameters and computation cost remain almost the same.

We conduct extensive experiments with various segmentation models on both PASCAL VOC 2012 [7] and Cityscapes [5] datasets. Our standard adversarial training strategy is effective to improve the robustness of semantic segmentation networks. Our new DDC-AT strategy further boost the effectiveness of defense. It yields superior performance under both white- and blackbox adversarial attack. Our main contribution is threefold.

- It is the first attempt (up to paper submission) to have comprehensive exploration on the effect of adversarial training for semantic segmentation. Our standard adversarial training can be treated as a strong baseline to evaluate defense strategies for semantic segmentation networks.

- We propose the DDC-AT to notably improve the defense performance of segmentation networks on both clean and adversarial samples.
- We conduct experiments with various model structures on different datasets, which manifest the effectiveness and generality of DDC-AT.

## 2 Related Work

**Adversarial Attack** Adversarial attack can be divided into two categories of white-box attack [2,8], where attackers have complete knowledge of the target model, and black-box attack [18,17], where attackers have almost no knowledge of the target model. Existing adversarial attack methods focus on solving image classification problems. Such attack is normally achieved by computing or simulating the gradient information of target models [8,22,6,12]. Meanwhile, as indicated by several recent papers [26,16,1], the semantic segmentation networks are also vulnerable to adversarial samples.

**Adversarial Defense** Current defense methods for classification task can be divided into four kinds. 1) Changing the input of networks to remove perturbation [10]. 2) Adopting random strategy to obtain correct output [25]. 3) Designing robust structures for different tasks [27]. 4) Adversarial training, which adds adversarial samples into training procedure [13,22,20]. No literature exists yet to improve robustness of semantic segmentation networks. Previous defense methods for semantic segmentation networks aim at the detection of adversarial regions [24]. However, detection only is not enough since the model still give incorrect prediction. We advocate that the model should accomplish correct output for adversarial samples during inference.

**Adversarial Training** Adversarial training can improve robustness of networks to a certain degree. Goodfellow et al. [8] first increased the robustness by feeding the model with both original and adversarial samples. Many researchers proposed follow-up work [13,22,3,11,23,28]. Due to the universality of adversarial training, we introduce it into the defense of semantic segmentation networks.

## 3 Attacking Semantic Segmentation

Given semantic segmentation network  $f$  and input  $x$ , the segmentation output is  $o = f(x)$ , where  $x \in \mathbb{R}^{H \times W \times 3}$  and  $o \in \mathbb{R}^{H \times W \times K}$  -  $H$ ,  $W$  and  $K$  are the height, width and number of classes respectively. For a clean sample  $x^{clean}$ , pixel  $x^{clean}(i, j)$  is called “clean pixel”; for the adversarial sample  $x^{adv}$ , which is obtained by adding perturbation on  $x^{clean}$ , pixel  $x^{adv}(i, j)$  is called “adversarial pixel”, paired with  $x^{clean}(i, j)$ . The standard cross-entropy loss is adopted as  $\mathcal{L}(f(x), y)$ , where  $y$  is the one-hot label of  $x$ .

Adversarial sample for  $f$  can be generated by computing the gradient information of  $f$  [1]. For example, given clean input  $x^{clean}$  and its one-hot label  $y$ , FGSM attack [8] perturbs  $x^{clean}$  as:

$$x^{adv} = x^{clean} + \epsilon \times \text{sign}(\nabla_{x^{clean}}(\mathcal{L}(f(x^{clean}), y))), \quad (1)$$

**Algorithm 1** Standard adversarial training

---

**Parameter:** clean training set  $\mathbf{X}$ , segmentation network  $f$ , maximum number of training iterations  $T_{max}$

- 1: Number of iteration  $T \leftarrow 0$
  - 2: **while**  $T \neq T_{max}$  **do**
  - 3:   Load a mini-batch of data  $\mathbf{D}_b = \{x_1^{clean}, \dots, x_m^{clean}\}$  from the training set  $\mathbf{X}$ .
  - 4:   Use  $f$  and the chosen attack to obtain adversarial samples  $\mathbf{A}_b = \{x_1^{adv}, \dots, x_m^{adv}\}$ .
  - 5:   Design the training batch as  $\{x_1^{clean}, \dots, x_{\lfloor m/2 \rfloor}^{clean}, x_{\lfloor m/2 \rfloor + 1}^{adv}, \dots, x_m^{adv}\}$  from  $\mathbf{D}_b$  and  $\mathbf{A}_b$ , and compute the loss for this training batch. Update parameters of the network  $f$  by back propagation.
  - 6:    $T \leftarrow T + 1$
  - 7: **end while**
- 

where  $x^{adv}$  is the resulting image with adversarial perturbation.  $\epsilon$  constrains the level of perturbation. Further, iterative adversarial attack would cause more serious threat. BIM [12] is such an approach – it has parameters for perturbation range  $\epsilon$ , step range  $\alpha$ , and start with  $x^{adv_0} = x^{clean} - \epsilon$  as:

$$x^{adv_{t+1}} = clip^\epsilon(x^{adv_t} + \alpha \times sign(\nabla_{x^{adv_t}}(\mathcal{L}(x^{adv_t}, y))), \quad (2)$$

where  $x^{adv_t}$  is the adversarial sample after the  $t$ -th attack step.

## 4 Standard Adversarial Training

We first design our standard adversarial training (SAT) on semantic segmentation task. We find that models trained with adversarial samples only largely drop performance on clean samples, and this leads to the phenomenon that the results on adversarial samples are better than those on clean samples. This phenomenon is called “label leaking” [13]. Models with “label leaking” are not suitable for the evaluation of robustness.

Thus, to ensure the performance on both clean/adversarial samples and avoid label leaking, we use mixed data where clean and adversarial samples are equally included in each batch during training. This mix strategy can scale up adversarial training to large models and datasets in classification [13]. It also works for semantic segmentation.

The detailed procedure of SAT is list in Alg. 1. This algorithm yields reasonable defense effect on various datasets and meets part of our requirement as the standard adversarial training.

## 5 Dynamic Divide-and-Conquer Adversarial Training

To further boost the robustness of semantic segmentation networks against adversarial samples, we propose a more effective dynamic divide-and-conquer adversarial training (DDC-AT) strategy in the following over SAT.

### 5.1 Divide-and-Conquer Procedure

DDC-AT adopts divide-and-conquer procedure during training, as shown in Fig. 2 (b) and explained as the following. 1) Divide: for an input image  $x$ , DDC-AT

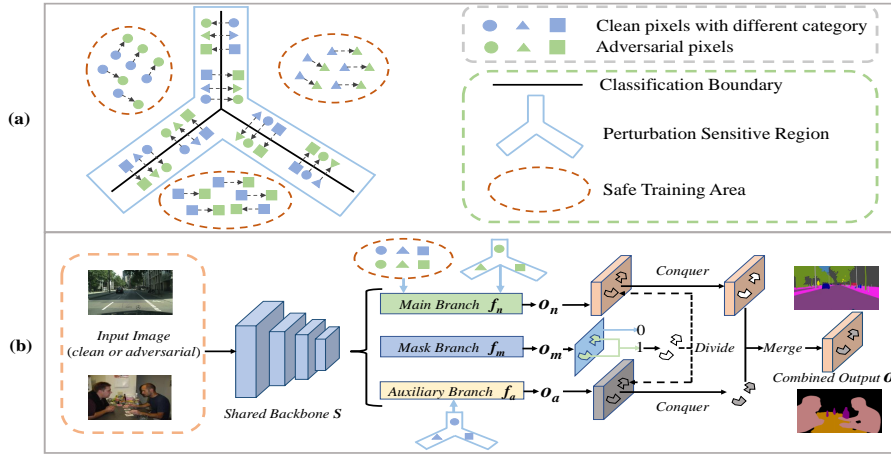


**Fig. 2.** Motivation and overall framework of DDC-AT. (a) Clean pixels in the output space are divided into two categories by divide-and-conquer strategy. (b) Main branch is utilized to conquer adversarial pixels, and clean pixels stay far away from classification boundary. The auxiliary branch is employed to conquer clean pixels that are sensitive to perturbation. The mask branch divides pixels into these two branches dynamically. The final output  $o$  is combined from the division during training. In testing, both auxiliary and mask branches are abandoned, and only main branch is utilized to output  $o_n$ .

divides its pixels into two sub-tasks for two branches respectively. 2) Conquer: each branch predicts labels for the pixels assigned to it. 3) Merge: predictions from two branches are merged into the overall prediction of image  $x$ .

**Dividing Pixels** As shown in Fig. 2 (a), clean pixels in output space can be divided into two types during training.

1) Clean pixels and their paired adversarial pixels are in the same classification space (in the Safe Training Area). The properties of clean and adversarial pixels are similar in this output space. They are likely to stay far away from the boundary. Their distribution can be aligned in an identical branch with adversarial training. We call such clean pixels, without boundary property,  $\mathcal{A}$ .

2) Paired clean and adversarial pixels are in diverse classification space. Such clean pixels are likely to stay near the classification boundary (in the Perturbation Sensitive Region). They have “boundary property” since they are easy to be perturbed through the boundary. Directly aligning them with the adversarial pixels in the identical branch is difficult, since the distribution is complex. Thus, we propose to first use two different branches to train them respectively. Once the clean and their adversarial pixels stay in the same space, we use an identical branch to align them. We call such clean pixels, with boundary property,  $\mathcal{B}$ .

In short, we divide pixels in one clean image into different kinds according to whether they have “boundary property”. The “boundary property” describes if clean pixels and the corresponding adversarial pixels have different predictions.

---

**Algorithm 2** Algorithm to obtain ground truth for training of mask branch  $f_m$

---

**Parameter:** clean data  $x^{clean}$ , one-hot label  $y$ , all-zero matrix  $\mathbf{0}$ , matrix function  $\mathcal{F} = \mathbf{1}[\mathcal{N}]$  ( $\mathcal{F}(i, j) = 1$  if  $\mathcal{N}(i, j)$  is True)

- 1: **Obtain** output  $o_n^{clean}$ ,  $o_a^{clean}$ , and  $o_m^{clean}$  for  $x^{clean}$  from  $f_n$ ,  $f_a$ , and  $f_m$  respectively. Obtain label map from  $o_m^{clean}$  as  $p^{clean}$ .
  - 2: **Compute** combined output  $o^{clean} = o_a^{clean} \odot p^{clean} + o_n^{clean} \odot (1 - p^{clean})$ , its label map is  $B^{clean}$ ,  $B^{clean}(i, j) \in \{0, 1, \dots, K - 1\}$ .
  - 3: **Use** loss  $\mathcal{L}(o_n^{clean}, y)$  to generate adversarial examples  $x^{adv}$ .
  - 4: **Obtain** output  $o_n^{adv}$ ,  $o_a^{adv}$ , and  $o_m^{adv}$  for  $x^{adv}$  from  $f_n$ ,  $f_a$ , and  $f_m$  respectively. Obtain label map from  $o_m^{adv}$  as  $p^{adv}$ .
  - 5: **Compute** combined output  $o^{adv} = o_a^{adv} \odot p^{adv} + o_n^{adv} \odot (1 - p^{adv})$  with label map  $B^{adv}$ , where  $B^{adv}(i, j) \in \{0, 1, \dots, K - 1\}$ .
  - 6: **Generate** “mask label” for  $x^{clean}$  as  $M^{clean} = \mathbf{1}[B^{clean} \neq B^{adv}]$ ,  $M^{clean} \in \mathbb{R}^{H \times W}$ .
  - 7: **Generate** “mask label” for  $x^{adv}$  as  $M^{adv} = \mathbf{0}$  with the same shape of  $M^{clean}$ .
  - 8: **return**  $M^{clean}$ ,  $M^{adv}$ ,  $x^{clean}$ , and  $x^{adv}$ .
- 

**Conquering Pixels** Based on the above division setting, we set our framework as shown in Fig. 2 (b), which consists of three branches. They are “main branch”, “auxiliary branch” and “mask branch”, denoted by  $f_n$ ,  $f_a$  and  $f_m$  respectively.  $f_n$  and  $f_a$  can be utilized to *conquer* pixels, i.e., predicting labels for pixels through forwarding the corresponding networks. We use “main branch” to conquer  $\mathcal{A}$ , as well as all adversarial pixels, and use “auxiliary branch” to conquer  $\mathcal{B}$ . In this way, clean pixels in one image after division can be processed by different branches. In additional,  $f_n$  and  $f_a$  have shared backbone, which means they help each other in the feature level. It is noteworthy that only the main branch is used for inference.

**Merging Pixels** As shown in Fig. 2 (b), divided pixels after conquering can be merged. This is because all pixels in one clean image are divided into  $f_n$  and  $f_a$ , and there is no overlap between the pixels assigned to  $f_n$  and  $f_a$ . Thus they can be merged into the final prediction of the input image to compute loss, according to the division. Moreover, this also indicates that the output space to decide the division should be the combination of  $f_n$  and  $f_a$  during training.

## 5.2 Dynamical Division and Implementation

In this section, we illustrate the dynamical property of division setting in DDC-AT, and explain how such division is achieved through unsupervised learning.

**Dynamical Division** During training,  $\mathcal{B}$  is first set to the auxiliary branch for training. Once such clean pixels turn into  $\mathcal{A}$ , they move to the main branch. Since the auxiliary branch is specially designed for the training of  $\mathcal{B}$ , it can remove boundary property for such clean pixels effectively to ensure that more clean pixels gradually move into the main branch.

In this design, the main branch finally trains all clean pixels to stay far away from the boundary. Such mechanism effectively helps avoid decrease of performance on clean samples. Moreover, training adversarial pixels with  $\mathcal{A}$  can improve the robustness towards adversarial perturbation for the main branch.

---

**Algorithm 3** Dynamic divide-and-conquer adversarial training for semantic segmentation networks

---

**Parameter:** clean training set  $\mathbf{X}$ , shared backbone  $S$ , main branch  $f_n$ , auxiliary branch  $f_a$ , mask branch  $f_m$ , training batch size  $m$ , and maximum training iteration  $T_{max}$   
 Number of iterations  $T \leftarrow 0$

- 1: **while**  $T \neq T_{max}$  **do**
  - 2: Load a mini-batch of data  $\mathbf{D}_b = \{x_1^{clean}, \dots, x_m^{clean}\}$  from  $\mathbf{X}$ , load their one-hot labels as  $\mathbf{Y}_b = \{y_1, \dots, y_m\}$ .
  - 3: Use current state of network  $\{S, f_n, f_a, f_m\}$ ,  $\mathbf{D}_b$ , and  $\mathbf{Y}_b$  in Alg. 2 to generate adversarial examples  $\mathbf{A}_b = \{x_1^{adv}, \dots, x_m^{adv}\}$ , and obtain “mask label” for  $\mathbf{D}_b$  and  $\mathbf{A}_b$  as  $\mathbf{M}_b^{clean} = \{M_1^{clean}, \dots, M_m^{clean}\}$  and  $\mathbf{M}_b^{adv} = \{M_1^{adv}, \dots, M_m^{adv}\}$ .
  - 4: Compute output from  $f_m$  for  $\mathbf{D}_b$ , and obtain the label map  $\{p_1^{clean}, \dots, p_m^{clean}\}$ .
  - 5: Compute output from  $f_m$  for  $\mathbf{A}_b$ , and obtain the label map  $\{p_1^{adv}, \dots, p_m^{adv}\}$ .
  - 6: Compute  $\{q_1^{clean}, \dots, q_m^{clean}\}$ , where  $q_i^{clean} = 1 - p_i^{clean}$ ;  
 Compute  $\{q_1^{adv}, \dots, q_m^{adv}\}$ , where  $q_i^{adv} = 1 - p_i^{adv}$ .
  - 7: Design training batch as  $\mathbf{T}_b = \{x_1^{clean}, \dots, x_{\lfloor m/2 \rfloor}^{clean}, x_{\lfloor m/2 \rfloor + 1}^{adv}, \dots, x_m^{adv}\}$ ,  
 $\mathbf{M}_b = \{M_1^{clean}, \dots, M_{\lfloor m/2 \rfloor}^{clean}, M_{\lfloor m/2 \rfloor + 1}^{adv}, \dots, M_m^{adv}\}$ ,  
 $\mathbf{P}_b = \{p_1^{clean}, \dots, p_{\lfloor m/2 \rfloor}^{clean}, p_{\lfloor m/2 \rfloor + 1}^{adv}, \dots, p_m^{adv}\}$ ,  
 $\mathbf{Q}_b = \{q_1^{clean}, \dots, q_{\lfloor m/2 \rfloor}^{clean}, q_{\lfloor m/2 \rfloor + 1}^{adv}, \dots, q_m^{adv}\}$ .
  - 8: Compute loss by Eqs. (3) and (4) with  $\mathbf{T}_b$ ,  $\mathbf{Y}_b$ ,  $\mathbf{P}_b$  and  $\mathbf{Q}_b$ . Update weights of network  $\{S, f_n, f_a\}$  by back propagation.
  - 9: Compute loss by Eq. (5) using  $\mathbf{T}_b$  and  $\mathbf{M}_b$ . Update weights of  $\{S, f_m\}$ .
  - 10:  $T \leftarrow T + 1$
  - 11: **end while**
- 

**Division Implementation via Unsupervised Learning** DDC-AT requires to distribute all adversarial pixels into  $f_n$ , and adopt dynamical division for clean pixels. Such division can be implemented by setting a “mask branch”  $f_m$ .

First,  $f_m$  predicts the division for pixels as shown in Fig. 2 (b). For input  $x$ , output from  $f_n$ ,  $f_a$ , and  $f_m$  is  $o_n$ ,  $o_a$ , and  $o_m \in \mathbb{R}^{H \times W \times 2}$  respectively. The label map of  $o_m$  is  $p \in \mathbb{R}^{H \times W}$ , which is a binary matrix to decide division.  $p(i, j) = 1$  means pixel  $x(i, j)$  is sent to  $f_a$ . Otherwise, it moves to  $f_n$ . This operation yields the combined output for  $x$  as  $o = o_a \odot p + o_n \odot (1 - p)$ , as shown in Fig. 2 (b). Here  $\odot$  is the Hadamard product. If  $x^{clean}$  is perturbed to  $x^{adv}$ , we denote the combined output as  $o^{clean}$  and  $o^{adv}$ , which are obtained in the same way.

Next, the ideal division scheme is based on these combined outputs. This scheme has a “mask label” notation  $M \in \mathbb{R}^{H \times W}$ .  $M(i, j) = 1$  means the pixel in  $(i, j)$  location is “divided into  $f_a$ ”. Otherwise, it is “divided into  $f_n$ ”. We set the mask label for  $x^{clean}$  as  $M^{clean}$ , and denote the label map of  $o^{clean}$  and  $o^{adv}$  as  $B^{clean}$  and  $B^{adv}$  respectively.

For pixel  $x^{clean}(i, j)$ , if  $B^{clean}(i, j) \neq B^{adv}(i, j)$ , it should set into  $f_a$  since it has the boundary property. In this case, we set  $M^{clean}(i, j) = 1$ . Otherwise, it should set into  $f_n$ , making  $M^{clean}(i, j) = 0$ . Besides, all adversarial pixels should be sent to  $f_n$ , and we set the mask label for  $x^{adv}$  as  $M^{adv} = \mathbf{0}$ .

$M^{adv}$  and  $M^{clean}$  are obtained according to the ideal division rule in DDC-AT. We can use them as the ground truth to train  $f_m$ . Repeating the whole process makes  $f_m$  learn how to achieve ideal division for pixels automatically. The pipeline to obtain  $M^{adv}$  and  $M^{clean}$  is listed in Alg. 2. Such training is unsupervised where learning of  $f_m$  does not need external supervised information.

In addition, since  $\mathcal{B}$  will be turned into  $\mathcal{A}$ , they will be assigned into main branch  $f_n$  progressively during training. Thus, the mask branch finally assigns all pixels into  $f_n$ , and the predicted mask has almost all zero values.

### 5.3 Overall Loss Function

For the training data  $x$  ( $x^{clean}$  or  $x^{adv}$ ), its label map obtained from the mask branch is  $p \in \mathbb{R}^{H \times W}$ , and we set  $q$  as  $q = 1 - p$ . The loss of  $x$  for  $f_n$  and  $f_a$  can be written as

$$\mathcal{L}_n = \mathbb{E} \left( - \sum_{i=0}^{K-1} [y_i \cdot \log(f_n(x)_i)] \odot q \right), \quad (3)$$

$$\mathcal{L}_a = \mathbb{E} \left( - \sum_{i=0}^{K-1} [y_i \cdot \log(f_a(x)_i)] \odot p \right), \quad (4)$$

where  $\mathbb{E}$  is the operation to compute the mean value.

Turn the mask label  $M$ , which is obtained in Alg. 2 for  $x$ , into one-hot form  $\widetilde{M}$ , we write the loss for  $f_m$  as

$$\mathcal{L}_m = \mathbb{E} \left( - \sum_{i=0}^1 [\widetilde{M}_i \cdot \log(f_m(x)_i)] \right). \quad (5)$$

Combined with Eqs. (3), (4) and (5), the overall loss term is

$$\mathcal{L}_{all} = \lambda_1 \mathcal{L}_n + \lambda_2 \mathcal{L}_a + \lambda_3 \mathcal{L}_m, \quad (6)$$

where  $\lambda_1$ ,  $\lambda_2$  and  $\lambda_3$  are all set to 1 in experiments. The overall training procedure is concluded in Alg. 3.

### 5.4 Superiority of Divide-and-Conquer

DDC-AT is designed to be superior than SAT and this is proved in the experiments part, in Sec. 6. It gets much better performance than classical SAT on both clean and adversarial pixels. We list the detailed explanation as below.

1) First, for the training of clean pixels in the main branch  $f_n$ , training with  $\mathcal{A}$  only (setting of DDC-AT) is much easier than mixed training with both  $\mathcal{A}$  and  $\mathcal{B}$  (setting of SAT). The introduced auxiliary branch  $f_a$  in DDC-AT can turn  $\mathcal{B}$  into  $\mathcal{A}$  gradually and effectively. Thus, the main branch  $f_n$  that is adopted for inference can better handle clean pixels and improve accuracy over SAT.

2) Second, to obtain decent results on adversarial pixels, SAT trains adversarial pixels with both  $\mathcal{A}$  and  $\mathcal{B}$ , while DDC-AT trains adversarial pixels with only  $\mathcal{A}$  for the main branch  $f_n$ . Obviously, training with both  $\mathcal{A}$  and  $\mathcal{B}$  causes higher difficulty for learning adversarial pixels than training with  $\mathcal{A}$  only. Thus, DDC-AT yields higher accuracy on adversarial pixels.

## 6 Experiments

### 6.1 Experimental Dataset

The newly proposed dynamic divide-and-conquer adversarial training (DDC-AT) strategy is effective for robust semantic segmentation. We use two representative datasets for the evaluation of semantic segmentation networks. They are PASCAL VOC 2012 [7] and Cityscapes [5] datasets.

**PASCAL VOC 2012** [7] dataset focuses on object segmentation. It contains 20 object classes and one background, with 1,464, 1,499 and 1,456 images for training, validation and testing respectively. The training set is augmented to 10,582 images in [9], which is also adopted in our work.

**Cityscapes** The Cityscapes [5] dataset is collected for urban scene understanding with 19 categories for semantic segmentation evaluation. It contains high quality pixel-level annotations with 2,975, 500 and 1,525 images for training, validation and testing respectively.

### 6.2 Training and Evaluation

**Training** We choose popular semantic segmentation architectures PSPNet [30] and DeepLabv3 [4] for experiments. We follow the hyper-parameters as suggested in [29] for all models. Both SAT and DDC-AT train networks with augmentation of adversarial samples, which are generated by a white-box BIM attacker. The main reason for choosing BIM is that we find models trained with single-step attack (e.g. FGSM) are more likely to introduce “label leaking” [13]. We however do not observe such phenomenon when trained with BIM.

**BIM Attacker** BIM is adopted as the form of untargeted attack [12]. The maximum perturbation value is set to  $\epsilon = 0.03 \times 255$  (by  $L_\infty$  constraint). The consideration is that perturbation can be visually noticed by human [1] with larger values. The attack step size and number of attack iterations are set as  $\alpha = 0.01 \times 255$  and  $n = 3$  for training respectively.

**Evaluation** We use the *mean of class-wise intersection over union* (mIoU) as our evaluation metric. The parameters  $\epsilon$  and  $\alpha$  are kept constant during training. For each training mini-batch, half of the input includes adversarial samples that are dynamically decided by current model states, resulting in variance of results. For both SAT and DDC-AT, we train for one more time and report the average results as well as their standard deviation.

### 6.3 Results on VOC

In this section, we evaluate SAT and DDC-AT on VOC dataset under both white- and black-box attack.

**White-Box Attack** In this attack, attackers utilize the exact gradient information of the target model [2]. For each model structure and dataset, we train SAT and DDC-AT to report the mean and standard deviation. Specifically, for the evaluation of robustness, we consider the number of BIM attack iteration number  $n$  ranging from 1 to 7.

**Table 1.** Evaluation under white-box attack on VOC. “No Defense” means normal training without adversarial samples. “clean” means mIoU on clean samples. Results in columns “1” to “7” are mIoUs under BIM attack with attack iteration number ranging from 1-7. “Mean” means the mean value of mIoU, and “Std” means the standard deviation of mIoU. The setting of “No Defense” is stable, thus we only report its mean value. Bold font is for the highest average performance.

	Methods	clean	Model: PSPNet						
			1	2	3	4	5	6	7
Mean	No Defense	0.769	0.371	0.189	0.111	0.078	0.062	0.054	0.048
	SAT	0.743	0.521	0.681	0.707	0.445	0.404	0.279	0.264
	DDC-AT	0.760	<b>0.535</b>	<b>0.756</b>	<b>0.723</b>	<b>0.479</b>	<b>0.470</b>	<b>0.338</b>	<b>0.332</b>
Std	SAT	0.005	0.042	0.018	0.008	0.029	0.032	0.032	0.032
	DDC-AT	0.001	0.005	0.005	0.005	0.022	0.040	0.040	0.046
	Methods	clean	Model: DeepLabv3						
			1	2	3	4	5	6	7
Mean	No Defense	0.775	0.374	0.196	0.119	0.081	0.064	0.055	0.048
	SAT	0.727	0.507	0.624	0.645	0.431	0.385	0.288	0.266
	DDC-AT	0.752	<b>0.518</b>	<b>0.699</b>	<b>0.678</b>	<b>0.436</b>	<b>0.447</b>	<b>0.323</b>	<b>0.326</b>
Std	SAT	0.010	0.040	0.006	0.010	0.019	0.020	0.020	0.010
	DDC-AT	0.001	0.006	0.013	0.011	0.005	0.030	0.012	0.020

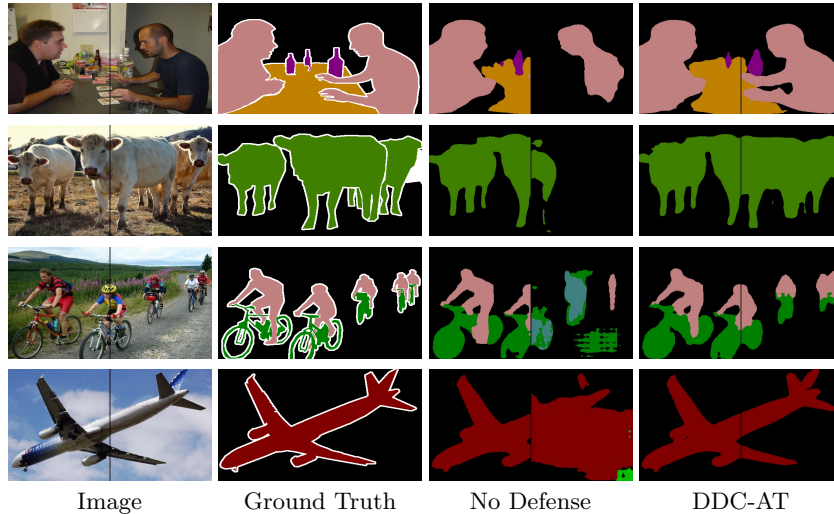


**Fig. 3.** Visual comparison on VOC. Top two rows are obtained from models with PSPNet, and bottom two rows are derived from models with DeepLabv3.

**White-Box Attack Results** The results of different defense methods on VOC are shown in Table 1. In this table, we compare our methods with the baseline (model trained with clean samples only, *i.e.*, no defense). Notably, without defense, BIM attack yields sharp performance decrease. Under untargeted attack setting, the results approach zeros when the attack iteration number is large.

Table 1 basically indicates that results on adversarial samples with large attack iteration number represent the lower bound of each method on adversarial perturbation, since the corresponding performance drops with the increase of  $n$ ,

**Table 2.** Evaluation under black-box attack on VOC. All symbolic representation has the same meaning as that of Table 1.

	Methods	clean	Model: PSPNet						
			1	2	3	4	5	6	7
Mean	No Defense	0.769	0.433	0.240	0.148	0.106	0.078	0.060	0.058
	SAT	0.743	0.584	0.565	0.535	0.513	0.471	0.449	0.415
	DDC-AT	0.760	<b>0.596</b>	<b>0.615</b>	<b>0.564</b>	<b>0.534</b>	<b>0.486</b>	<b>0.461</b>	<b>0.437</b>
Std	SAT	0.005	0.032	0.029	0.027	0.028	0.027	0.042	0.041
	DDC-AT	0.001	0.021	0.017	0.017	0.018	0.031	0.039	0.040
	Methods	clean	Model: DeepLabv3						
			1	2	3	4	5	6	7
Mean	No Defense	0.775	0.445	0.246	0.148	0.105	0.083	0.070	0.064
	SAT	0.727	0.567	0.518	0.518	0.510	0.470	0.450	0.431
	DDC-AT	0.752	<b>0.583</b>	<b>0.604</b>	<b>0.547</b>	<b>0.526</b>	<b>0.483</b>	<b>0.460</b>	<b>0.436</b>
Std	SAT	0.010	0.023	0.038	0.033	0.037	0.040	0.041	0.050
	DDC-AT	0.001	0.020	0.051	0.035	0.018	0.017	0.016	0.016

and converges when  $n$  is large (actually, the mean value of mIoU does not change more than 0.025 when  $n$  is 10 or 20, compared with the results when  $n=7$ ). This leads to the conclusion that SAT is already reasonable: it improves results from 0.048 to 0.264 on PSPNet and 0.048 to 0.266 on DeepLabv3 when  $n = 7$ . Further, the standard deviation of SAT is low, which means SAT is stable.

DDC-AT in Table 1 gives results of our final framework. Performance of DDC-AT on clean samples increases compared with SAT (by 0.017 and 0.025 on PSPNet and DeepLabv3 respectively), consistent with our design motivation.

Further, the performance of DDC-AT is higher than SAT notably under each attacker iteration on average. Intriguingly, the best case of SAT under every attack iteration is almost the worst case of DDC-AT. For example, when the attack iteration  $n = 3$ , we have  $0.707 + 0.008 < 0.723 - 0.005$  on PSPNet and  $0.645 + 0.010 < 0.678 - 0.011$  on DeepLabv3.

More interestingly, for unseen attack, DDC-AT clearly improves robustness over SAT. Small standard deviation for DDC-AT indicates that results are stable. We also provide visual comparison on VOC in Fig. 3 for comparing result quality.

**Black-Box Attack** Black-box attackers cannot utilize the exact gradient information of the target model. Instead, gradient information from a substitute network, which is defensively trained on the same dataset [18,17,14], can be adopted. In our evaluation setting, the perturbation for trained PSPNet models is generated by DeepLabv3, trained on the same dataset and enhanced with adversarial training, and vice versa. For SAT and DDC-AT, the substitute networks are the same for fair comparison.

As described in Sec. 6.2, models trained with the same method and dataset may have diverse behavior. To reduce evaluation bias from training randomness, we evaluate SAT and DDC-AT on dataset  $\hat{D}$  in the following way. Using training strategy  $\hat{S}$  (SAT or DDC-AT) with model structure  $\hat{f}$  on  $\hat{D}$ , we obtain model set  $\hat{M}_1$ . Then using adversarial training with model structure different from  $\hat{f}$  on  $\hat{D}$ , we obtain model set  $\hat{M}_2$  as substitute defensive networks. Finally, for each model in  $\hat{M}_1$ , we use attack generated from each model in  $\hat{M}_2$  for evaluation.

**Table 3.** Performance comparison of defense setting in ablation study on VOC. Symbolic representation is the same as that of Table 1.

	Methods	clean	Model: PSPNet						
			1	2	3	4	5	6	7
Mean	SAT	0.743	0.521	0.681	0.707	0.445	0.404	0.279	0.264
	DDC-AT-M	0.751	0.511	0.690	0.690	0.441	0.463	0.304	0.318
	DDC-AT-N	0.748	0.528	0.737	0.694	0.456	0.460	0.318	0.330
	DDC-AT	0.760	<b>0.535</b>	<b>0.756</b>	<b>0.723</b>	<b>0.479</b>	<b>0.470</b>	<b>0.338</b>	<b>0.332</b>
	Methods	clean	Model: DeepLabv3						
			1	2	3	4	5	6	7
Mean	SAT	0.727	0.507	0.624	0.645	0.431	0.385	0.288	0.266
	DDC-AT-M	0.741	0.505	<b>0.720</b>	0.666	<b>0.451</b>	0.435	0.314	0.304
	DDC-AT-N	0.741	0.506	0.683	0.665	0.426	0.415	0.312	0.302
	DDC-AT	0.752	<b>0.518</b>	0.699	<b>0.678</b>	0.436	<b>0.447</b>	<b>0.323</b>	<b>0.326</b>

**Black-Box Attack Results** Results under black-box evaluation on VOC are included in Table 2. Performance of clean models also decreases along with the increase of attack iteration, like the white-box situation. This phenomenon suggests that there is strong transferability for adversarial samples in the semantic segmentation task. It is therefore meaningful to evaluate robustness under this black-box setting.

In comparison between DDC-AT and SAT, we use the same hyper-parameters as white-box attacks. From Table 2, it is clear that SAT also improves the defense effect. The standard deviation of SAT is larger than the results by white-box attacks because black-box perturbation for each model is obtained from a set of substitute networks, which have different adversarial behaviors.

The final performance of DDC-AT is consistently higher than SAT with attack iteration number ranging from 1 to 7. Meanwhile, the standard deviation of our method is lower in all cases, especially under unseen attack. It proves that DDC-AT is more stable and effective than SAT by all types of attack.

#### 6.4 Ablation Study

The motivation of DDC-AT is to dynamically divide pixels with/without boundary property into diverse branches during training. We prove our division setting is better than other alternatives by adjusting the division setting for pixels with boundary property. The common alternatives are the following.

- Use “main branch” to deal with pixels from clean and adversarial samples without boundary property. Use “auxiliary branch” to process pixels from clean and adversarial samples with boundary property. We name this setting DDC-AT-M.
- Use “main branch” to deal with pixels from clean samples, pixels from adversarial samples without boundary property. Use “auxiliary branch” to solve pixels from adversarial samples with boundary property. We name this setting DDC-AT-N.
- Use only “main branch” to deal with pixels from either clean or adversarial samples. This is what SAT does, thus we do not train the mask branch.

**Table 4.** Results on clean samples of Cityscapes.

	Method	PSPNet	DeepLabv3
Mean Value	No Defense	0.746	0.748
	SAT	0.690	0.694
	DDC-AT	0.717	0.713
Standard Deviation	SAT	0.010	0.010
	DDC-AT	0.001	0.003

**Table 5.** Evaluation of our method and the baseline under black-box attack on Cityscapes. Symbolic representations are same as Table 1.

	Methods	Model: PSPNet						
		1	2	3	4	5	6	7
Mean	No Defense	0.476	0.280	0.141	0.069	0.039	0.033	0.022
	SAT	0.511	0.444	0.399	0.367	0.320	0.308	0.291
	DDC-AT	<b>0.561</b>	<b>0.506</b>	<b>0.425</b>	<b>0.379</b>	<b>0.339</b>	<b>0.323</b>	<b>0.306</b>
Std	SAT	0.005	0.030	0.026	0.033	0.023	0.026	0.025
	DDC-AT	0.004	0.010	0.010	0.010	0.002	0.002	0.002
	Methods	Model: DeepLabv3						
		1	2	3	4	5	6	7
Mean	No Defense	0.482	0.299	0.153	0.076	0.044	0.031	0.024
	SAT	0.507	0.432	0.394	0.361	0.328	0.316	0.297
	DDC-AT	<b>0.523</b>	<b>0.478</b>	<b>0.416</b>	<b>0.378</b>	<b>0.341</b>	<b>0.328</b>	<b>0.311</b>
Std	SAT	0.008	0.030	0.028	0.030	0.022	0.023	0.025
	DDC-AT	0.006	0.019	0.010	0.010	0.004	0.003	0.004

For all these methods, only main branch is utilized during testing. We evaluate the performance of these alternatives and list results in Table 3. For PSPNet model, the performance of DDC-AT-N is higher than SAT and lower than DDC-AT. The average results of DDC-AT-M are comparable with SAT and are worse than DDC-AT. Similarly, for DeepLabv3 model, the average results of DDC-AT-M and DDC-AT-N are lower than DDC-AT, and higher than SAT consistently. In summary, the division setting of DDC-AT is optimal among these common alternatives. We include the detailed visual illustration and the standard deviation of results for these alternatives in the supplementary material.

## 6.5 Results on Cityscapes

**White-Box Attack** Results of different methods on clean samples are included in Table 4. DDC-AT effectively reduces drop of performance on clean samples, compared with SAT. In fact, DDC-AT improves mIoU on clean samples by 0.027 and 0.023, which are significant with the setting of PSPNet and DeepLabv3, compared with SAT. The results of DDC-AT are also more stable over SAT.

We show results of different defense methods under white-box attack on Cityscapes dataset in Fig. 4. Obviously, clean models get worse with the increase of attack iterations, like the case in VOC, which proves general effect of adversarial attack for different datasets. The results of DDC-AT and SAT

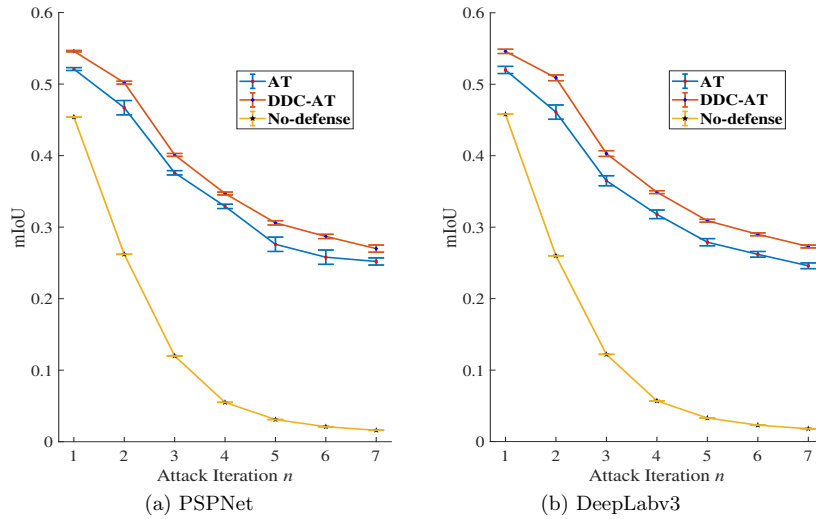


**Fig. 4.** Results under white-box attack on Cityscapes, which are plotted by lines (for mean values) with error bars (denoting standard deviation).

under various attack iterations are like we observe before – they also improve robustness of the models on this large dataset. DDC-AT outperforms SAT in Fig. 4 where the best cases of SAT under every attack iteration are actually worse than the worst cases of DDC-AT. The deviation in Fig. 4 indicates that both DDC-AT and SAT are stable, while DDC-AT is even better.

**Black-Box Attack** The results under the evaluation of black-box attack for the Cityscapes dataset are shown in Table 5. DDC-AT also outperforms SAT on average with different attack iterations. The standard deviation of DDC-AT is still strictly smaller than that of SAT. For example, when  $n = 5 \sim 7$ , the standard deviation of SAT is larger than 0.020 for both PSPNet and DeepLabv3, while standard deviation of DDC-AT is smaller than 0.005.

## 7 Conclusion

In this paper, we have explored the property of adversarial training on the semantic segmentation task. Our defense strategy can consistently enhance the robustness of target models under adversarial attack. Besides proposing the standard adversarial training (SAT) process, we propose a new strategy to improve the performance of adversarial training in this task, with no extra parameter and computation cost introduced during inference. The extensive experimental results with different model structures on two representative benchmark datasets suggest that the proposed method achieves significantly better generalization and stability on unseen adversarial examples and clean samples, compared with standard adversarial training and other alternatives.

## References

1. Arnab, A., Miksik, O., Torr, P.H.: On the robustness of semantic segmentation models to adversarial attacks. In: CVPR (2018)
2. Athalye, A., Carlini, N.: On the robustness of the cvpr 2018 white-box adversarial example defenses. arXiv:1804.03286 (2018)
3. Cai, Q.Z., Du, M., Liu, C., Song, D.: Curriculum adversarial training. IJCAI (2018)
4. Chen, L.C., Papandreou, G., Schroff, F., Adam, H.: Rethinking atrous convolution for semantic image segmentation. arXiv:1706.05587 (2017)
5. Cordts, M., Omran, M., Ramos, S., Rehfeld, T., Enzweiler, M., Benenson, R., Franke, U., Roth, S., Schiele, B.: The cityscapes dataset for semantic urban scene understanding. In: CVPR (2016)
6. Dong, Y., Liao, F., Pang, T., Su, H., Zhu, J., Hu, X., Li, J.: Boosting adversarial attacks with momentum. In: CVPR (2018)
7. Everingham, M., Van Gool, L., Williams, C.K., Winn, J., Zisserman, A.: The pascal visual object classes (voc) challenge. IJCV (2010)
8. Goodfellow, I.J., Shlens, J., Szegedy, C.: Explaining and harnessing adversarial examples. ICLR (2014)
9. Hariharan, B., Arbeláez, P., Girshick, R., Malik, J.: Hypercolumns for object segmentation and fine-grained localization. In: CVPR (2015)
10. Jia, X., Wei, X., Cao, X., Foroosh, H.: Comdefend: An efficient image compression model to defend adversarial examples. In: CVPR (2019)
11. Kannan, H., Kurakin, A., Goodfellow, I.: Adversarial logit pairing. arXiv:1803.06373 (2018)
12. Kurakin, A., Goodfellow, I., Bengio, S.: Adversarial examples in the physical world. ICLR (2016)
13. Kurakin, A., Goodfellow, I., Bengio, S.: Adversarial machine learning at scale. ICLR (2016)
14. Liu, Y., Chen, X., Liu, C., Song, D.: Delving into transferable adversarial examples and black-box attacks. arXiv:1611.02770 (2016)
15. Madry, A., Makelov, A., Schmidt, L., Tsipras, D., Vladu, A.: Towards deep learning models resistant to adversarial attacks. arXiv:1706.06083 (2017)
16. Metzen, J.H., Kumar, M.C., Brox, T., Fischer, V.: Universal adversarial perturbations against semantic image segmentation. In: ICCV (2017)
17. Papernot, N., McDaniel, P., Goodfellow, I.: Transferability in machine learning: from phenomena to black-box attacks using adversarial samples. arXiv:1605.07277 (2016)
18. Papernot, N., McDaniel, P., Goodfellow, I., Jha, S., Celik, Z.B., Swami, A.: Practical black-box attacks against machine learning. In: Proceedings of the 2017 ACM on Asia conference on computer and communications security (2017)
19. Papernot, N., McDaniel, P., Jha, S., Fredrikson, M., Celik, Z.B., Swami, A.: The limitations of deep learning in adversarial settings. In: 2016 IEEE European Symposium on Security and Privacy (2016)
20. Song, C., He, K., Wang, L., Hopcroft, J.E.: Improving the generalization of adversarial training with domain adaptation. ICLR (2018)
21. Szegedy, C., Zaremba, W., Sutskever, I., Bruna, J., Erhan, D., Goodfellow, I., Fergus, R.: Intriguing properties of neural networks. arXiv:1312.6199 (2013)
22. Tramèr, F., Kurakin, A., Papernot, N., Goodfellow, I., Boneh, D., McDaniel, P.: Ensemble adversarial training: Attacks and defenses. ICLR (2017)

23. Wang, J., Zhang, H.: Bilateral adversarial training: Towards fast training of more robust models against adversarial attacks. In: ICCV (2019)
24. Xiao, C., Deng, R., Li, B., Yu, F., Liu, M., Song, D.: Characterizing adversarial examples based on spatial consistency information for semantic segmentation. In: ECCV (2018)
25. Xie, C., Wang, J., Zhang, Z., Ren, Z., Yuille, A.: Mitigating adversarial effects through randomization. ICLR (2017)
26. Xie, C., Wang, J., Zhang, Z., Zhou, Y., Xie, L., Yuille, A.: Adversarial examples for semantic segmentation and object detection. In: CVPR (2017)
27. Xie, C., Wu, Y., Maaten, L.v.d., Yuille, A.L., He, K.: Feature denoising for improving adversarial robustness. In: CVPR (2019)
28. Zhang, H., Wang, J.: Defense against adversarial attacks using feature scattering-based adversarial training. In: NIPS (2019)
29. Zhao, H.: semseg. <https://github.com/hszhao/semseg> (2019)
30. Zhao, H., Shi, J., Qi, X., Wang, X., Jia, J.: Pyramid scene parsing network. In: CVPR (2017)